ACS Photonics

Article

pubs.acs.org/journal/apchd5

Observation of Asymmetric Nanoscale Optical Cavity in GaAs Nanosheets

Shermin Arab,[†,‡] P. Duke Anderson,[†,‡] Chun-Yung Chi,[†,‡] P. Daniel Dapkus,[†,§,∥,‡] Michelle L. Povinelli,[†,‡] and Stephen B. Cronin*[,†,§,‡]

[†]Department of Electrical Engineering, [§]Department of Physics, [∥]Department of Chemical Engineering and Materials Science, and [‡]Center for Energy Nanoscience, University of Southern California, Los Angeles, California 90089, United States

Supporting Information

ABSTRACT: GaAs nanosheets with no twin defects, stacking faults, or dislocations are excellent candidates for optoelectrical applications. Their outstanding optical behavior and twin free structure make them superior to traditionally studied GaAs nanowires. While many research groups have reported optically resonant cavities (i.e., Fabry−Perot) in 1D nanowires, here, we report an optical cavity resonance in GaAs nanosheets consisting of complex 2D asymmetric modes, which are fundamentally different from one-dimensional cavities. These resonant modes are detected experimentally using photoluminescence (PL) spectroscopy, which exhibits a series of peaks or "fringes" superimposed on the bulk GaAs photoluminescence spectrum. Finite-difference time-domain (FDTD) simulations confirm these experimental findings and provide a detailed picture of these complex resonant modes. Here, the complex modes of this cavity are formed by the three nonparallel edges of the GaAs nanosheets. Due to the asymmetrical nature of the nanosheets, the mode profiles are largely unintuitive. We also find that by changing the substrate from Si/SiO_2 to Au, we enhance the resonance fringes as well as the overall optical emission by 5× at room temperature. Our FDTD simulation results confirm that this enhancement is caused by the local field enhancement of the Au substrate and indicate that the thickness of the nanosheets plays an important role in the formation and enhancement of fringes.

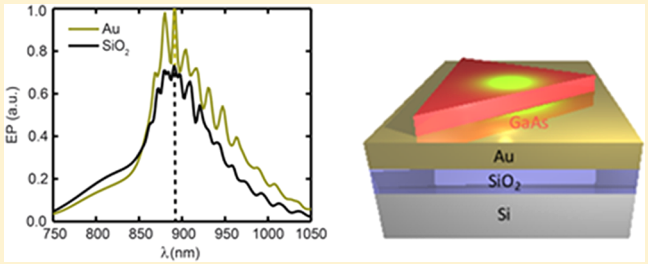

KEYWORDS: *MOCVD, GaAs, nanosheet, nanowires, photoluminescence*

GaAs nanostructures are among the best candidates for optoelectrical applications including solar cells, LEDs, and lasers.[1−5] However, these structures, particularly nanowires, suffer from various defects, such as twin formation, dislocations, and stacking faults. While GaAs nanowires suffer from such defects, nanosheets grow easily without twin defects or stacking faults;[6] hence, overall they show higher quality and optical properties in comparison to GaAs nanowires.[7] Nanoscale lasers have been studied in a variety of nanostructure geometries. So far, both nanowire lasers and thin film semiconductors have demonstrated high intensity emission under optical or electrical pumping.[1−5] Duan et al. reported electrically pumped lasing from *n*-type CdS nanowires.[2] Fukui et al. reported observation of Fabry-Perrot (FP) resonances and later lasing from GaAs nanowires.[3,8,9] Most recently, Saxena et al.[10] reported passivated GaAs nanowire lasing at room temperature by optimizing the size and surface passivation. In our previous work, we demonstrated enhanced FP resonance from GaAs nanowires at room temperature through surface passivation with wide band gap semiconductor AlGaAs and also ionic liquid electrolyte.[11] Since the original paper reporting nanowire lasing,[2] much of the effort in this area has been focused on reducing the effects of defects and impurities in order to improve the optoelectronic properties of these nanomaterials.

In the work presented here, we investigate GaAs nanosheets, which have demonstrated improved crystal structure over nanowires and present a new morphology for optically resonant devices and systems. This same general approach was previously applied by our group to GaAs nanowires.[11] However, the results observed from 2D nanosheets are nonintuitive. It should be noted that a vast majority of previous papers reporting on optical cavity resonances in nanoscale systems are reported in 1D nanowires and 2D photonic crystals, although similar observations in non-nanoscale regime have been studied.[12−14] Traditional photonic crystals require difficult nanofabrication techniques,[15,16] and the 2D nanosheets provide a new platform for achieving 2D resonances without the need for complex nanofabrication. The *Q*-factor reported for artificially fabricated PCs are usually in a higher range (10^5 and higher) in comparison to the optical cavity formed here; however, we believe after AlGaAs passivation, these GaAs nanosheets can provide higher *Q*-factors.[17] The GaAs nanosheet optical cavities may also be compared to triangular-shaped lasers reported previously.[18,19] However, in most cases, the triangular lasers are formed from heterostructures or

Received: April 7, 2015
Published: July 13, 2015

DOI: 10.1021/acsphotonics.5b00179
ACS Photonics 2015, 2, 1124−1128

superlattices. In general, the nonradiative recombination processes are well-controlled in triangular lasers, which lead to higher quality factors and longer carrier lifetimes; both of which result in higher emissions and lower lasing thresholds.

Most previous studies report one-dimensional cavities formed either between two parallel mirrors or between the two end facets of a nanowire. In the work presented here, we demonstrate an in-plane (2D) optical cavity formed by the three nonparallel edges of the GaAs nanosheets. The nature of this resonance is studied using photoluminescence (PL) spectroscopy as a function of the GaAs nanosheet dimensions, laser power, temperature, and underlying substrate. In order to obtain a fundamental understanding of the resonances and underlying PL enhancement mechanism, finite-difference time-domain (FDTD) simulations are carried out on an individual GaAs nanosheet. The simulations are configured to separate various enhancement mechanisms of light absorption and emission. Optical cavity modes are visualized by plotting the electric field intensity through a cross-sectional slice of the nanosheet. Both the strength and quality factors of the resonances are extracted from measurements and calculations. Formation of such cavities provide a path toward the development of room-temperature 2D nanolasers. An optically pumped, cost-effective nanolaser with reduced footprint could be used in optical communications.

GaAs nanosheets are synthesized on (111)B GaAs substrates by metal organic chemical vapor deposition (MOCVD) with selective area growth (SAG). The detailed synthesis method has been described in previous publications.[7,20] Briefly, trimethylgallium (TMGa) and arsine are used as precursors for Ga and As deposition, and nanosheets are *n*-type doped using disilane (Si_2H_6). A 28 nm layer of SiN_x is deposited on the GaAs substrate using plasma enhanced chemical vapor deposition (PECVD), which serves as the growth mask. Electron beam lithography is used to create nanoscale strips in the SiN_x, which is selectively etched, leading to the formation of windows exposing the underlying GaAs substrate. The nanosheets are grown in a hydrogen environment at 0.1 atm using a V/III ratio of 1.5 and Ga/Si ratio of about 16000 for 30 min at 790 °C. The partial pressure of TMGa, AsH_3, and Si_2H_6 are 1.124×10^{-6}, 1.63×10^{-6}, and 2.857×10^{-9} atm, respectively. The as-grown nanosheets are sonicated for 5 s in isopropanol and subsequently transferred onto Si/SiO_2 (300 nm SiO_2) or Si/SiO_2/Au (300 nm- SiO_2/200 nm Au) substrates. These GaAs nanosheets grow on (111)B surfaces through a self-terminating growth mechanism, which results in their triangular shape with a base length of 6−10 μm, and height of 2−4 μm, as shown in Figure 1a. The thickness of these nanostructures is 200 ± 25 nm. Micro-Raman and photoluminescence spectroscopy are collected using a 40× objective lens, an 1800 L/mm grating, and a silicon CCD camera to detect the photoluminescence (PL) in the range from 750 to 950 nm. Low to moderate power excitation (10^2−10^5 mW/cm^2) using a 532 nm laser is used to avoid optical heating.

Figure 1a shows an SEM image of a GaAs nanosheet deposited on a Si/SiO_2 substrate. The thickness of the nanosheet is measured using atomic force microscopy (AFM), which gives a measured value of 200 ± 20 nm. The center of the sample is excited by a 532 nm CW laser focused to a spot size of 1.5 μm with an excitation power of 10^5 mW/cm^2. The corresponding PL spectrum taken at 77 K is shown in Figure 1b. The spacing between the resonance peaks varies

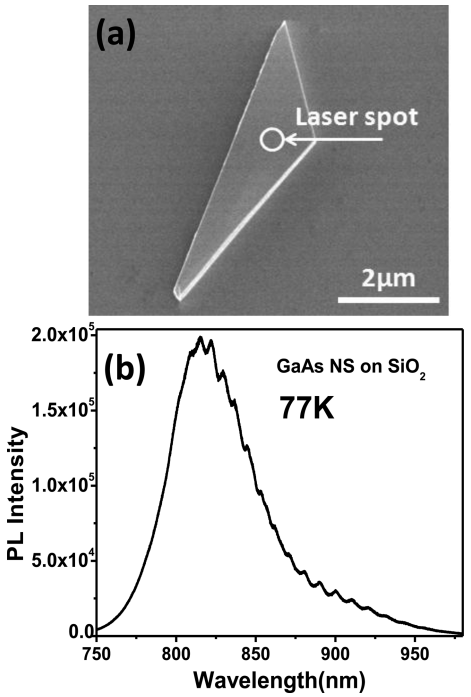

Figure 1. (a) SEM image of a GaAs nanosheet and (b) photoluminescence spectrum taken at 77 K. The dominant peak at 816 nm is attributed to the band-to-band transition, and the peak at 860 nm corresponds to carbon acceptor impurities.

between 6.5 and 10 nm, with an average spacing of 8.5 nm. In this spectrum, two predominant peaks are observed at 1.52 and 1.44 eV. The peak at 1.52 eV corresponds to the nominal band gap of GaAs (1.507 eV at 77 K), blueshifted by 12 meV due to the *n*-type doping by Si dopant impurities, which results in Pauli blocking of band-edge to band-edge optical transitions. The 1.44 eV sub-band gap peak is attributed to an acceptor-band transition arising from carbon impurities originating from the metalorganic precursors of the MOCVD growth.[21,22] The quality factors of the resonance peaks range from 88 to 125, indicating that trapped light is totally internally reflected roughly 100 times. These resonance fringes are only observed in nanosheets with thickness of 200−220 nm, whereas no such resonance is observed in thicker GaAs (see Figure S1 in the Supporting Information). These values of the *Q*-factor and optimal thicknesses are quite similar to those of GaAs nanowires described in our previous work.[11] Table 1 lists a comparison of resonance parameters between nanowires and nanosheets. It is remarkable that the *Q*-factors of the nanosheets are on the same order of magnitude as in the nanowires, considering that there are no parallel facets in the nanosheet. We have observed the highest PL intensity for the case where the polarization direction is parallel to the base of

Table 1. Comparison of Resonance Parameters for GaAs Nanowires and Nanosheets

	GaAs nanowires	GaAs nanosheets
peak-to-peak spacing (experimental)	8−10 nm	6.5−10 nm
peak-to-peak spacing (theoretical)	11 nm	12.3 nm
quality factor	181	125
optimal thickness	270 nm ±20 nm	210 nm ±10 nm

DOI: 10.1021/acsphotonics.5b00179
ACS Photonics 2015, 2, 1124−1128

the NS and the lowest for the case where the polarization is perpendicular to the base.

In Figure 2, the PL spectra of a similar GaAs nanosheet deposited on a Si/SiO_2/Au (200 nm of Au deposited on Si/SiO_2) substrate is compared to that of one taken on Si/SiO_2 without Au. For both data sets, the PL spectra are centered at 840 nm, corresponding to a band gap of 1.47 eV. Here, we observe a blueshift of 50 meV compared to the room temperature GaAs band gap (1.42 eV), again due to n-type doping of GaAs with Si. It should be noted that this spectra is taken at room temperature and, hence, the blue-shift seen in Figure 1b is not observed. While the fringes appear less sharp in comparison to the measurement at 77 K, the peak-to-peak spacing is consistent. A 5× enhancement in the PL intensity and emergence of fringes are observed as a result of the Au substrate. Here, the metallic substrate does not behave as a simple reflector, since the expected enhancement of a mirror would only be on the order of 2×. The effective cavity length can be determined using the following formula and the experimental value of the peak-to-peak spacing:

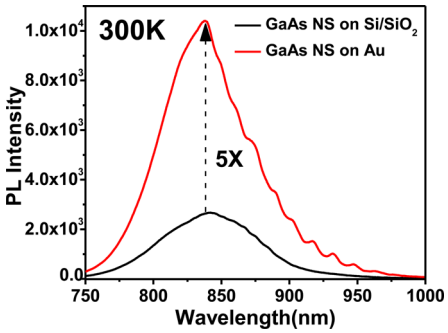

Figure 2. Photoluminescence spectra from GaAs nanosheets on Si/SiO_2 and Si/SiO_2/Au. Spectra were collected at room temperature under 532 nm CW laser excitation.

$$\Delta\lambda = \frac{\lambda^2}{2L\left[n - \lambda\left(\frac{dn}{d\lambda}\right)\right]}$$

Assuming n = 3.655, $\Delta\lambda$ = 10.8 nm, and $dn/d\lambda = -0.822/\mu m$, the cavity length is approximately 7.45 μm, consistent with the base length of the nanosheet. As a comparison to our previous work, the Fabry−Perot resonance observed in GaAs nanowires grown by MOCVD exhibited a mode spacing of 11.5 nm (at 4 K).[11]

In order to understand the underlying optical resonances and PL enhancement mechanism, finite-difference time-domain (FDTD) simulations are carried out on a GaAs nanosheet on top of both Si/SiO_2 and Si/SiO_2/Au substrates, as illustrated in Figure 3a,b. In each configuration, the geometry of the nanosheet resembles those grown experimentally, with dimensions determined from SEM and AFM. The simulated nanosheet is an obtuse triangle with a maximum base length of 6 μm, an obtuse angle of 119.5°, minimum angle of 21.8°, and thickness of 200 nm. In each system, we account for the dispersive nature of the materials and impose perfectly matched layers (PML) along the simulation boundaries. A 532 nm optical pump, indicated by the green spot in each figure, is focused onto the GaAs nanosheet. We simulate the pump excitation using a Gaussian beam with a 1.5 μm spot size.

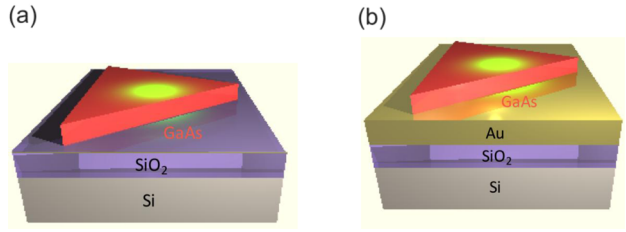

Figure 3. Schematic diagrams illustrating the two simulated pump geometries: GaAs nanosheet on top of (a) 300 nm of SiO_2 and a semi-infinite Si substrate and (b) 200 nm of Au on top of 300 nm of SiO_2 and a semi-infinite Si substrate. The nanosheet has a maximum side length of 6 μm, obtuse angle of 119.5°, minimum angle of 21.8°, and a thickness of 200 nm. The green spot in each diagram represents a 532 nm optical pump with a beam waist of 1.5 μm focused onto the nanosheet.

We can quantify the power *absorbed* in each system using the following formula:

$$P_{ABS} = 1/2\omega |\vec{E}|^2 \varepsilon''$$

where ω is the angular frequency, $|\vec{E}|^2$ is the electric-field intensity, and ε'' is the imaginary component of the dielectric function. In order to calculate the absorptive enhancement in the GaAs nanosheet due to the presence of an underlying Au film, we take a horizontal slice across the triangular profile of the nanosheet (100 nm above the SiO_2 and Au substrates), integrate the electric-field intensity, and take the corresponding ratio. The absorptive enhancement factor (EF_{ABS}) for a single wavelength is simply the ratio of the integrated electric-field intensities:

$$EF_{ABS} = \frac{\int |\vec{E}_{Au}|^2 dA}{\int |\vec{E}_{SiO_2}|^2 dA}$$

With the pump excitation at 532 nm, the absorptive enhancement factor is nearly 11.5×, indicating that the Au substrate leads to 11.5× more optical absorption within the nanosheet. Here, the metallic film appears to form a vertical cavity with the top of the nanosheet that traps light and results in a large absorptive enhancement factor.

We model PL *emission* within the GaAs nanosheet using electric dipole sources. Each electric dipole emits between 750 and 1050 nm. A Gaussian distribution is superimposed upon the emission spectra so that the results more closely resemble the PL data collected experimentally. In order to examine the impact of the emitter position on the observed optical resonances, we consider four emitter positions: one position near each corner of the nanosheet and one position near its center. At each emitter position, we consider three orthogonal polarizations (i.e., x, y, and z). In order to avoid coherence effects, we include one dipole per simulation and later perform an incoherent summation of the emission results.

We introduce a quantity, the extracted power (EP), which is defined as the total power collected from the top of the GaAs nanosheet, measured using a flux-plane monitor. Figure 4a shows the incoherently summed EP results for the cross-sectional position located near the smallest corner of the nanosheet. Optical fringes are clearly visible in the simulated spectra for both the SiO_2 and Au underlying substrate. Emission characteristics relating to the remaining three emitter positions are described in the Supporting Information. Figure 4b shows the electric-field intensity patterns for the wave-

DOI: 10.1021/acsphotonics.5b00179
ACS Photonics 2015, 2, 1124−1128

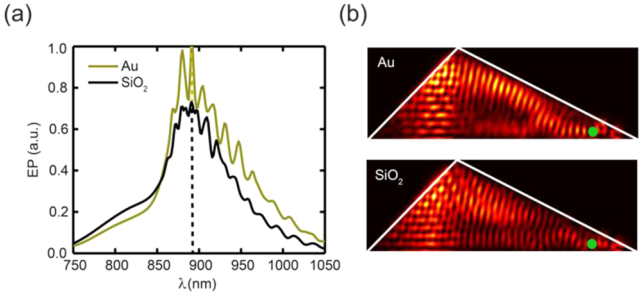

Figure 4. (a) Incoherently summed extracted power (EP) spectra calculated for the topologies shown in Figure 3. (b) Electric-field patterns for resonances in each material system; the wavelength of each resonance is indicated by the dashed lines in (a). The solid white lines indicate the triangular outline of the nanosheet, whereas the green dots indicate the position of the dipole emitters.

lengths corresponding to the dashed line in Figure 4a, which coincides with a resonance in each system. The solid white outline marks the triangular boundary of the nanosheet, whereas the green dot indicates the position of the dipole emitters. The nanosheet forms an in-plane cavity with clear interference fringes evident in the 2D field intensity plots, further supporting the presence of resonant modes.

The integrated extracted power enhancement (EP_{ENH}) is defined as

$$EP_{ENH} = \frac{\int EP_{Au} d\lambda}{\int EP_{SiO_2} d\lambda}$$

and represents the comparative enhancement in collected emission due to the Au film. We find that this enhancement is independent of the emitter's position (see Supporting Information, Figure S2) with a value always near unity. The broadband EP enhancement for the emission results shown in Figure 4a is 1.2×. If we consider the overall PL enhancement to be a product of absorptive enhancement and extracted power (EP) enhancement, then we theoretically predict a PL enhancement of nearly 13.8×. The majority of the enhancement contribution is owed to absorptive enhancement, resulting from the formation of a vertical cavity due to the underlying metallic film. The observation of optical resonances, however, is a consequence of the in-plane cavity formed by the cross-sectional profile of the nanosheet. Both the number and quality-factor of observed resonances is strongly dependent on the emitter's position (see Supporting Information).

In conclusion, we report the observation of an optical resonance in GaAs nanosheets resulting from the formation of an asymmetric cavity created by the nonparallel edges of these nanostructures. The optical resonance is seen experimentally in the photoluminescence spectra of the nanosheets, as a series of peaks of fringes observed on top of the normal photoluminescence spectrum of bulk GaAs. The resonance consist of complex in-plane modes resulting from total internal reflections within the nanosheet itself, as seen in the electric field intensity profiles calculated by finite-difference time-domain simulations. *Q*-factors of 125 are observed in these nanosheets, which is comparable to previous measurements of GaAs nanowires. By changing the underlying substrate from Si/SiO_2 to $Si/SiO_2/Au$, a 5× enhancement in the PL intensity and resonance fringes is observed in these GaAs nanosheets. This substrate-induced PL enhancement is also seen in our FDTD simulations, which indicate that the enhancement is primarily due to absorptive enhancement rather than photoemission enhancement. The overall theoretical enhancement due to both absorptive and extracted power is predicted to be 13.8× and does not include any losses due to nonradiative recombination effects.

■ ASSOCIATED CONTENT

Supporting Information

Details on FDTD calculations for electric field intensity and absorptive enhancement as the function of thickness for different substrates are provided. Extracted power and FP resonances are demonstrated for different material systems. The Supporting Information is available free of charge on the ACS Publications website at DOI: 10.1021/acsphotonics.5b00179.

■ AUTHOR INFORMATION

Corresponding Author

*E-mail: scronin@usc.edu.

Notes

The authors declare no competing financial interest.

■ ACKNOWLEDGMENTS

This material is based on work supported as part of the Center for Energy Nanoscience (CEN), an Energy Frontier Research Center (EFRC) funded by the U.S. Department of Energy, Office of Science and Office of Basic Energy Sciences, under Award DE-SC0001013. Computing resources were provided by the USC Center for High Performance Computing and Communications.

■ REFERENCES

(1) Chu, S.; Wang, G.; Zhou, W.; Lin, Y.; Chernyak, L.; Zhao, J.; Kong, J.; Li, L.; Ren, J.; Liu, J. Electrically pumped waveguide lasing from ZnO nanowires. *Nat. Nanotechnol.* **2011**, *6*, 506−510.

(2) Duan, X.; Huang, Y.; Agarwal, R.; Lieber, C. M. Single-nanowire electrically driven lasers. *Nature* **2003**, *421*, 241−245.

(3) Yang, L.; Motohisa, J.; Fukui, T.; Jia, L. X.; Zhang, L.; Geng, M. M.; Chen, P.; Liu, Y. L. Fabry-Perot microcavity modes observed in the micro-photoluminescence spectra of the single nanowire with InGaAs/GaAs heterostructure. *Opt. Express* **2009**, *17*, 9337−9346.

(4) Cho, S.; Ma, J.; Kim, Y.; Sun, Y.; Wong, G. K.; Ketterson, J. B. Photoluminescence and ultraviolet lasing of polycrystalline ZnO thin films prepared by the oxidation of the metallic Zn. *Appl. Phys. Lett.* **1999**, *75*, 2761−2763.

(5) Yu, P.; Tang, Z.; Wong, G. K.; Kawasaki, M.; Ohtomo, A.; Koinuma, H.; Segawa, Y. Room-temperature gain spectra and lasing in microcrystalline ZnO thin films. *J. Cryst. Growth* **1998**, *184*, 601−604.

(6) Chi, C. Y.; Chang, C. C.; Hu, S.; Yeh, T. W.; Cronin, S. B.; Dapkus, P. D. Twin-Free GaAs Nanosheets by Selective Area Growth: Implications for Defect-Free Nanostructures. *Nano Lett.* **2013**, *13*, 2506−2515.

(7) Chang, C.-C.; Chi, C.-Y.; Chen, C.-C.; Huang, N.; Arab, S.; Qiu, J.; Povinelli, M. L.; Dapkus, P. D.; Cronin, S. B. Carrier dynamics and doping profiles in GaAs nanosheets. *Nano Res.* **2014**, *7*, 163−170.

(8) Hua, B.; Motohisa, J.; Ding, Y.; Hara, S.; Fukui, T. Characterization of Fabry-Perot microcavity modes in GaAs nanowires fabricated by selective-area metal organic vapor phase epitaxy. *Appl. Phys. Lett.* **2007**, *91*, 131112.

(9) Hua, B.; Motohisa, J.; Kobayashi, Y.; Hara, S.; Fukui, T. Single GaAs/GaAsP coaxial core− shell nanowire lasers. *Nano Lett.* **2009**, *9*, 112−116.

(10) Saxena, D.; Mokkapati, S.; Parkinson, P.; Jiang, N.; Gao, Q.; Tan, H. H.; Jagadish, C. Optically pumped room-temperature GaAs nanowire lasers. *Nat. Photonics* **2013**, *7*, 963−968.

DOI: 10.1021/acsphotonics.5b00179
ACS Photonics 2015, 2, 1124−1128

(11) Arab, S.; Anderson, P. D.; Yao, M.; Zhou, C.; Dapkus, P. D.; Povinelli, M. L.; Cronin, S. B. Enhanced Fabry-Perot resonance in GaAs nanowires through local field enhancement and surface passivation. *Nano Res.* **2014**, *7*, 1146−1153.
(12) Marinace, J.; Michel, A.; Nathan, M. Triangular injection lasers. *Proc. IEEE* **1964**, *52*, 722−723.
(13) Behfar-Rad, A.; Ballantyne, J.; Wong, S. AlGaAs/GaAs-based triangular-shaped ring ridge lasers. *Appl. Phys. Lett.* **1992**, *60*, 1658−1660.
(14) Nöckel, J. U.; Stone, A. D. Ray and wave chaos in asymmetric resonant optical cavities. *arXiv:chao-dyn/9806017* **1998**, 10.1038/385045a0.
(15) Camargo, E.; Chong, H.; De La Rue, R. 2D photonic crystal thermo-optic switch based on AlGaAs/GaAs epitaxial structure. *Opt. Express* **2004**, *12*, 588−592.
(16) Herrmann, R.; Sünner, T.; Hein, T.; Löffler, A.; Kamp, M.; Forchel, A. Ultrahigh-quality photonic crystal cavity in GaAs. *Opt. Lett.* **2006**, *31*, 1229−1231.
(17) Arab, S.; Chi, C.-Y.; Shi, T.; Wang, Y.; Dapkus, D. P.; Jackson, H. E.; Smith, L. M.; Cronin, S. B. Effects of Surface Passivation on Twin-Free GaAs Nanosheets. *ACS Nano* **2015**, *9*, 1336−1340.
(18) Chang, H.; Kioseoglou, G.; Lee, E.; Haetty, J.; Na, M.; Xuan, Y.; Luo, H.; Petrou, A.; Cartwright, A. Lasing modes in equilateral-triangular laser cavities. *Phys. Rev. A: At., Mol., Opt. Phys.* **2000**, *62*, 013816.
(19) Ando, S.; Kobayashi, N.; Ando, H. Triangular-facet lasers coupled by a rectangular optical waveguide. *Japanese journal of applied physics* **1997**, *36*, L76.
(20) Chi, C.-Y.; Chang, C.-C.; Hu, S.; Yeh, T.-W.; Cronin, S. B.; Dapkus, P. D. Twin-free GaAs nanosheets by selective area growth: Implications for defect-free nanostructures. *Nano Lett.* **2013**, *13*, 2506−2515.
(21) Kushibe, M.; Eguchi, K.; Funamizu, M.; Ohba, Y. Heavy carbon doping in metalorganic chemical vapor deposition for GaAs using a low V/III ratio. *Appl. Phys. Lett.* **1990**, *56*, 1248−1250.
(22) Kohda, H.; Wada, K. The carbon doping mechanism in GaAs using trimethylgallium and trimethylarsenic. *J. Cryst. Growth* **1996**, *167*, 557−565.

DOI: 10.1021/acsphotonics.5b00179
ACS Photonics 2015, 2, 1124−1128